The iron and nickel spectra measured with CALET on the International Space Station

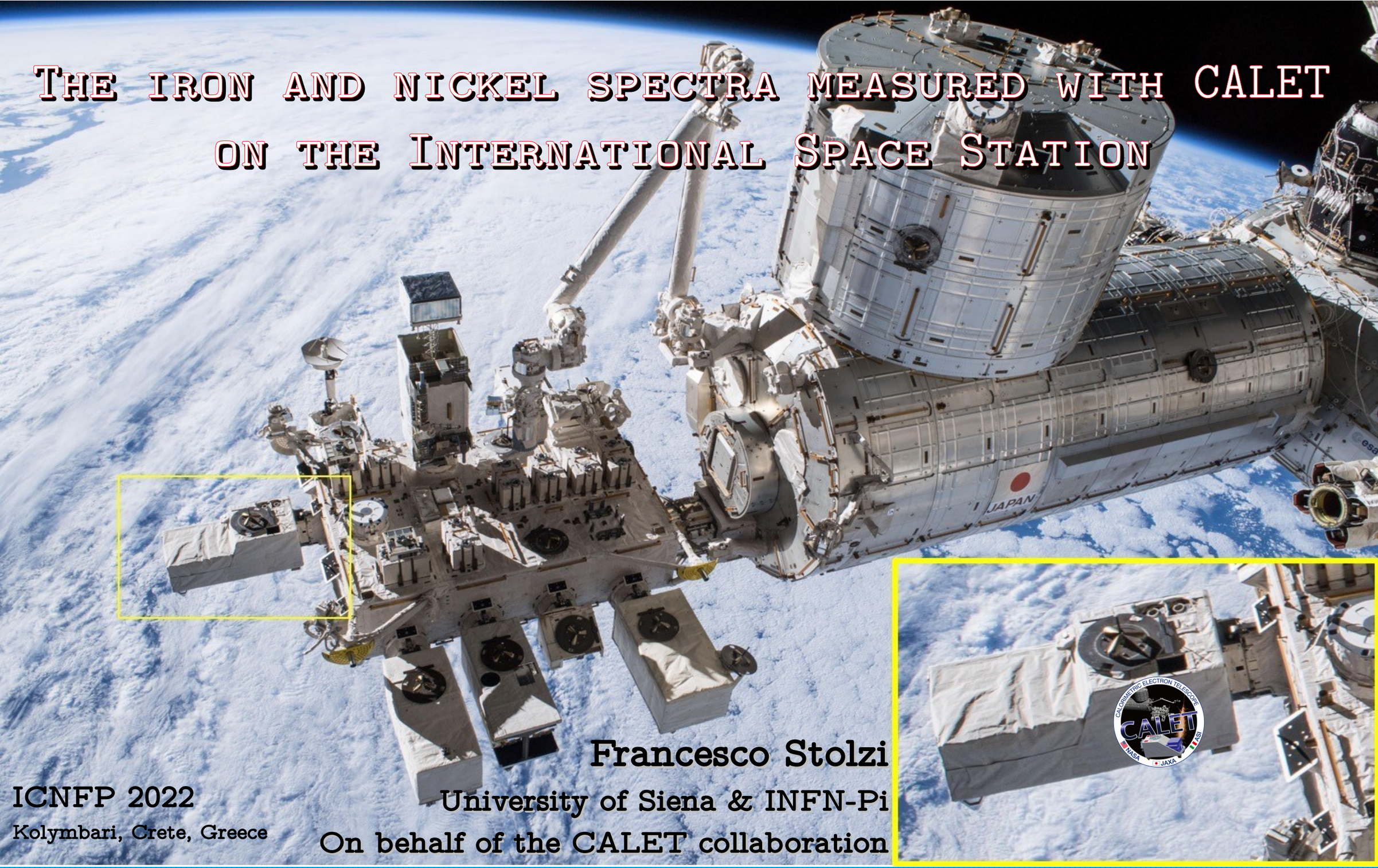

Francesco Stolzi
University of Siena & INFN-Pi
On behalf of the CALET collaboration

ICNFP 2022
Kolymbari, Crete, Greece

CALET PAYLOAD

CALET launch on Aug. 19th, 2015 on Japanese H2-B rocket

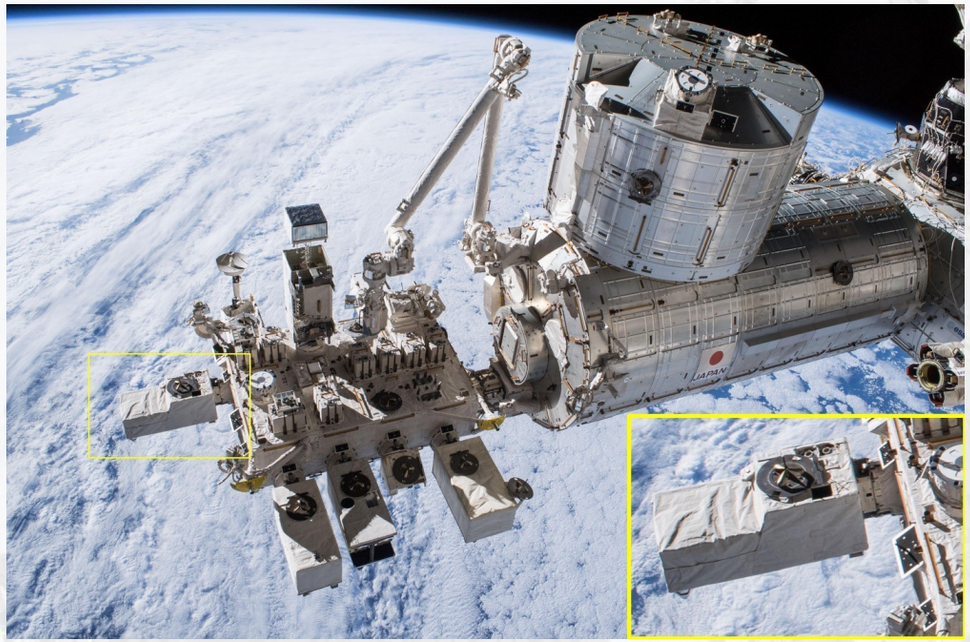

CALET was emplaced on Japanese Experiment Module – Exposed Facility (JEM-EF) port#9 on Aug. 25th, 2015

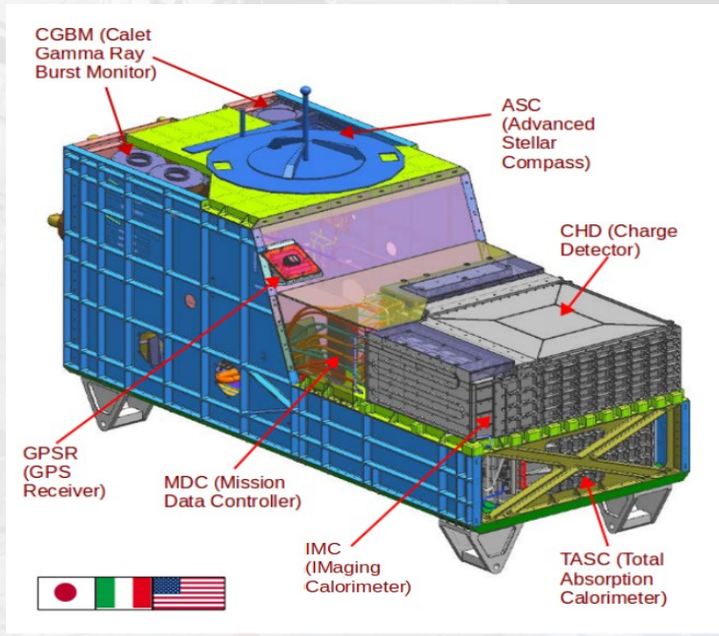

JEM Standard Payload
Mass: 612.8 kg
Size: 1850 mm (L) x 800 mm (W) x 1000 mm (H)
Power Consumption: 507 W (max)

CALET started scientific observations on Oct. 13Th, 2015. More than 3.4 billion events collected so far.

CALET INSTRUMENT

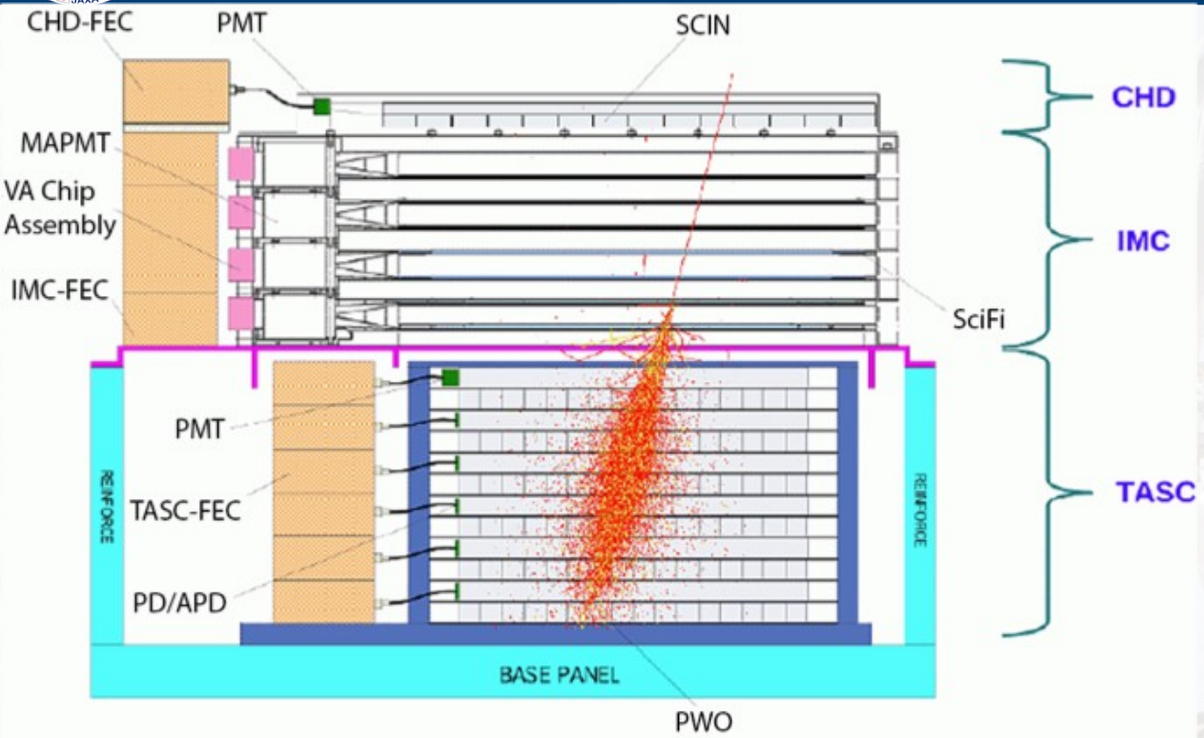

A 30 radiation length deep calorimeter designed to detect electrons and gammas up to 20 TeV and cosmic rays up to 1 PeV

	CHD (Charge Detector)	IMC (Imaging Calorimeter)	TASC (Total Absorption Calorimiter)
Measure	Charge $(1 \leq Z \leq 40)$ $\Delta Z/Z = 0.15$ for C, 0.35 for Fe	*Particle ID*, Tracking ΔX at CHD = 300 μm	Energy, *Dynamic range: 1 –10^6 MIP (1 GeV –1 PeV)*
Geometry/ Material	Plastic Scintillator 14 paddles x 2 layers (X,Y) Paddle size: 32 mm x 10 mm x 450 mm	Scintillating fibers 448 x 16 (X,Y) 7 W layers, total thickness: 3 X_0 Scifi Size: 1 mm^2 x 448 mm	16 PWO *logs* x 12 layers (X,Y) Total thickness: 27 X_0, 1.2 λ_I Log size: 19 mm x 20 mm x 326 mm
Readout	PMT + CSA	64-anode MAPMT + ASIC	APD/PD + CSA PMT + CSA (for trigger)

Nuclei observation with CALET

One of main objectives is the precise measurement of the transition region for each nuclear species and extension to TeV energy → Spectral hardening

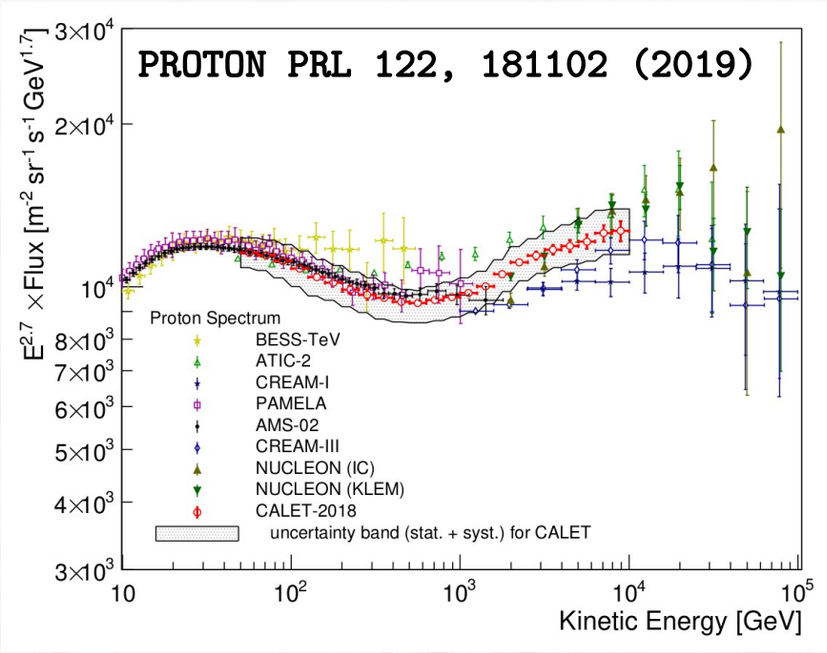

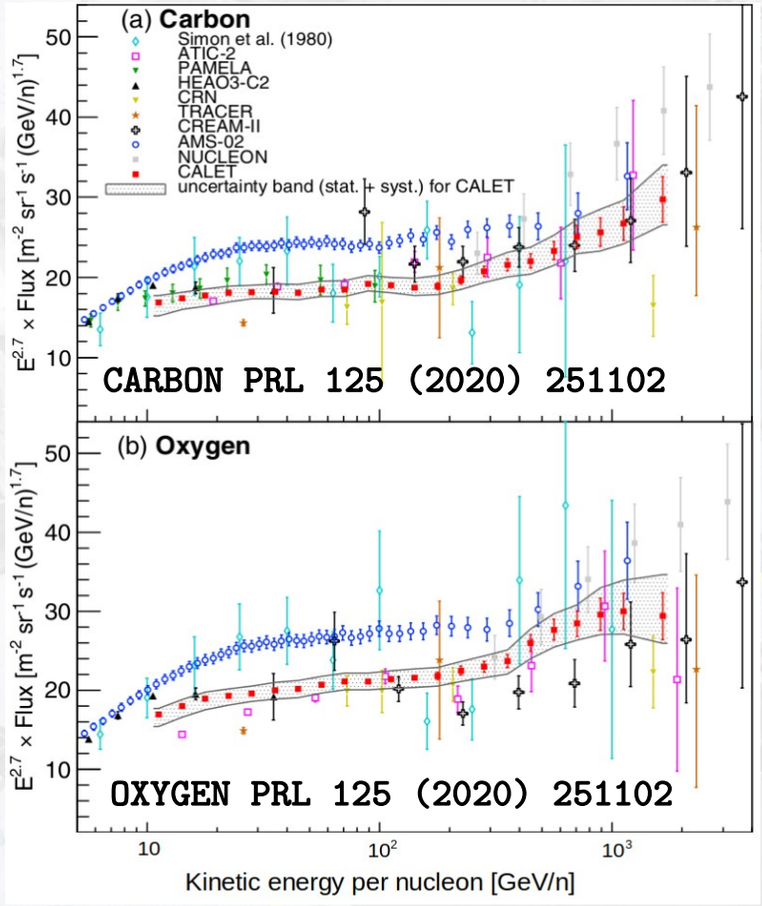

Energy spectra of proton, C and O indicate the spectral hardening at a few 100 GeV/n.

What about havier nuclei?

Iron and Nickel Analysis procedure

(1) Data sample

- ✔ ***Iron:*** from January 2016 to May 2020, 1613 *d*, live time $T = 3.3 \times 10^4$ *h*, 85.8% total obs. time.
- ✔ ***Nickel:*** from November 2015 to May 2021, 2038 *d*, live time $T = 4.1 \times 10^4$ *h*, 86% total obs. time.
- ✔ MC simulations based on EPICS.

(2) Shower event selection and High Energy Trigger (HET)

- ✔ Select interacting particles.

(3) Tracking with IMC

- ✔ Identify the impact point and the particle's direction.

(4) Acceptance cut

- ✔ ***Iron:*** events crossing the whole detector from the top of the CHD to the TASC bottom layer and clear from the edges of TASCX1 and of the bottom TASC layer by at least 2 cm ($S\Omega \sim 416\ cm^2\ sr$).
- ✔ ***Nickel:*** extended acceptance, no condition on the TASC bottom layer ($S\Omega \sim 510\ cm^2\ sr$).

(5) Charge consistency with CHD

- ✔ Remove particles undergoing a charge-changing interaction in the upper part of the instrument.

(6) Charge selection with CHD

- ✔ ***Iron:*** candidates are identified by an ellipse centered at $Z = 26$.
- ✔ ***Nickel:*** candidates are identified by an ellipse centered at Z = 28.

(7) Background estimation

(8) Energy unfolding

(9) Systematic errors

(10) Flux measurement

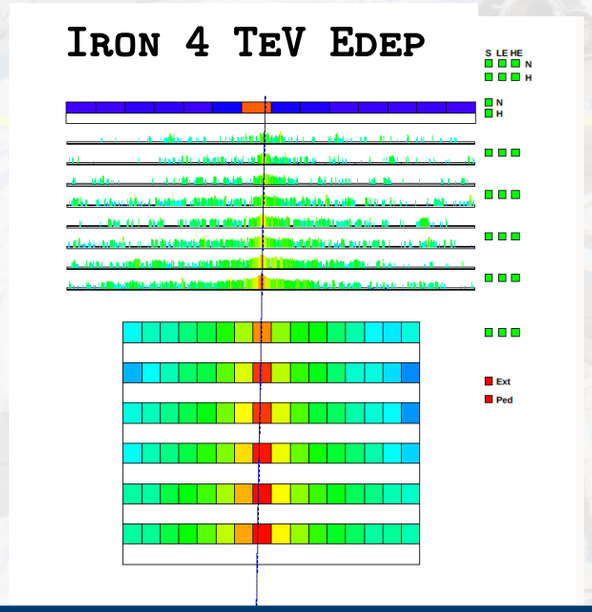

(5) (6) Charge identification

Charge Z reconstructed by measuring the ionization deposits in the CHD

- Non linear response to Z^2 due to the quenching effect in the scintillators is corrected using a "halo" model.

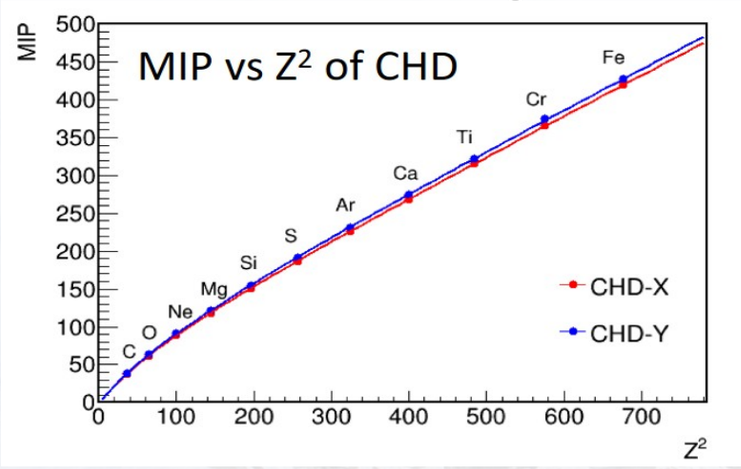

- In order to remove background events interacting in CHD a Charge Consistency Cut is applied: $|Z_{CHDX}-Z_{CHDY}|<1.5$
- Charge resolution σ_Z are 0.35 *e* and 0.39 *e* for Fe and Ni respectively.

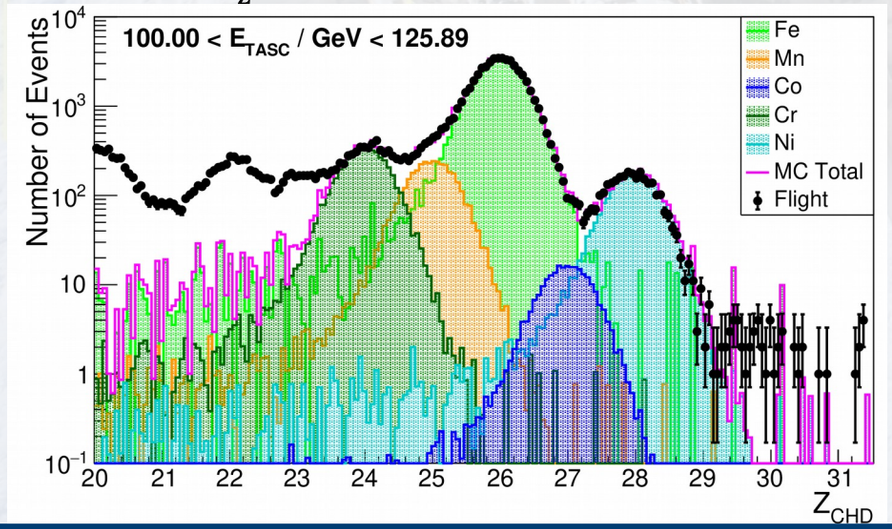

- Iron (nickel) events are selected within an ellipse centered at Z = 26 (28), with $1.25\sigma_x$ ($1.4\sigma_x$) and $1.25\sigma_y$ ($1.4\sigma_y$) wide semiaxes for Z_{CHDX} and Z_{CHDY}, respectively, and rotated clockwise by 45°

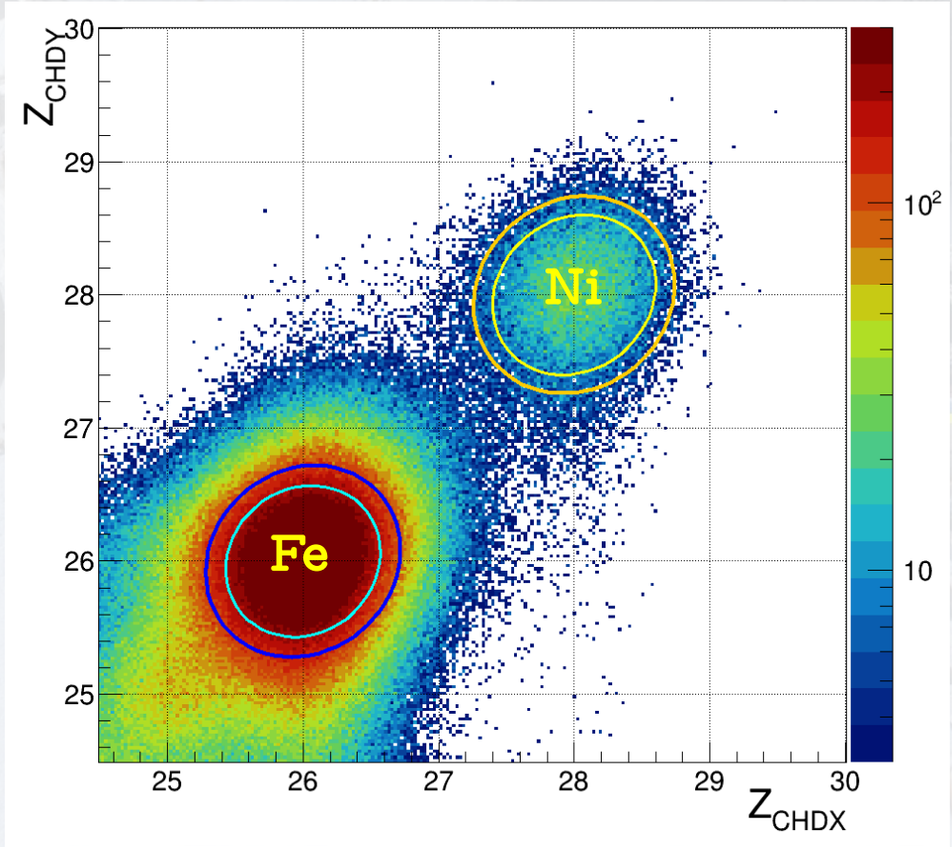

(7) Fe dN/dEdep and background estimate

dN/dEdep distributions for Fe, Mn, Co, Cr, Ni after Fe selection

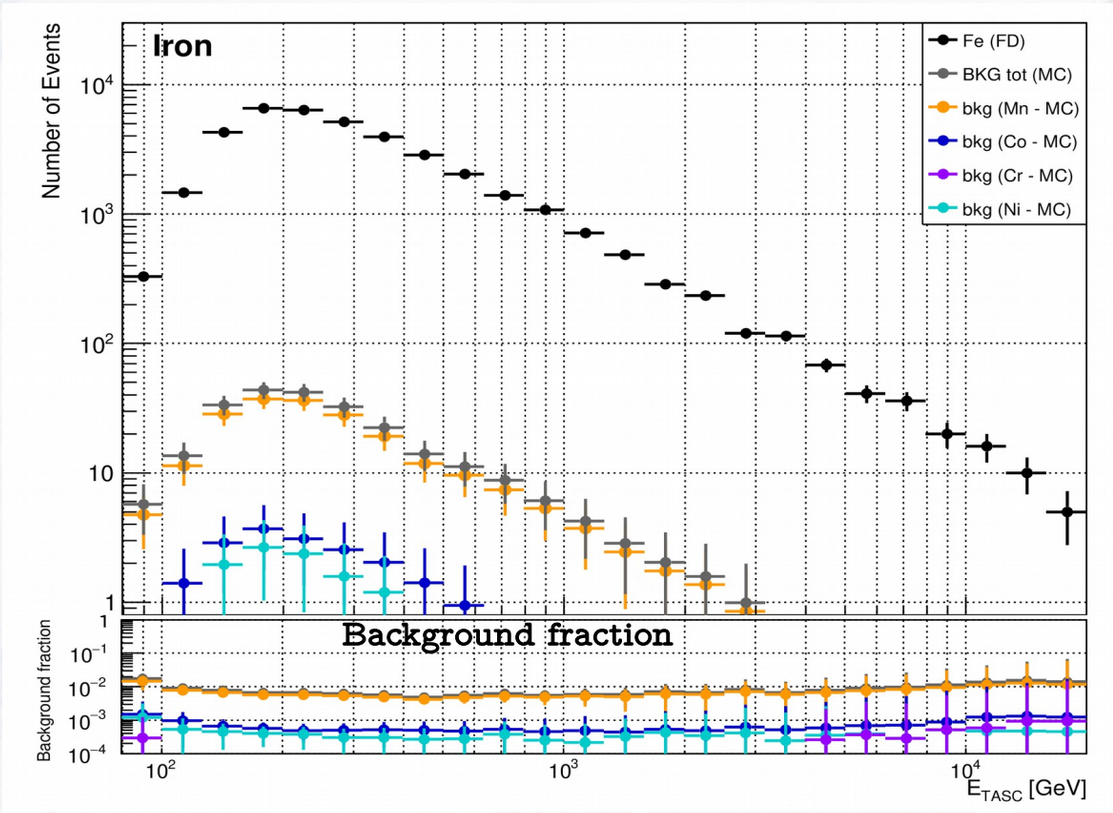

dN/dEdep distributions for Ni, Co, Fe after Ni selection

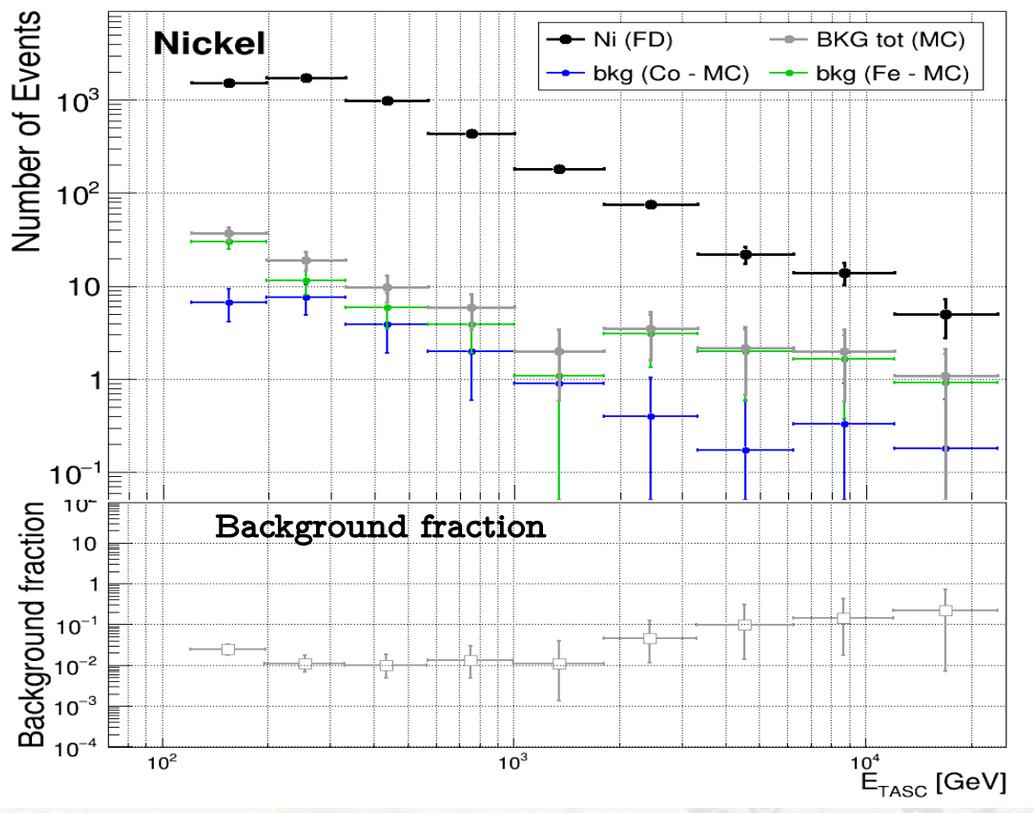

Background contamination from different nuclear species misidentified as Fe (Ni) are estimated by Monte Carlo simulation.

- Iron: total background is few percent in all energy bins.
- Nickel: ~ 1% between 10^2 and 10^3 GeV, up to 10% at 10^4 GeV

(8) Energy Unfolding

- Relatively limited calorimetric energy resolution for hadrons (of the order of~30%)

- Energy unfolding is applied to correct for bin-to-bin migration effect and obtain the primary energy spectrum

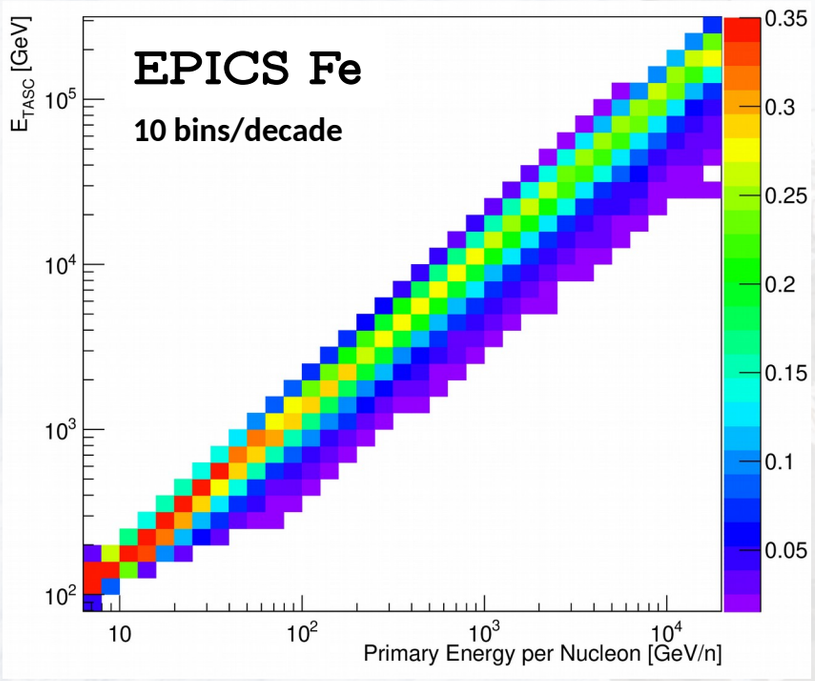

In the figures the color scale is associated to the probability that iron (nickel) candidates in a given bin of kinetic energy cover different intervals of E_{TASC}

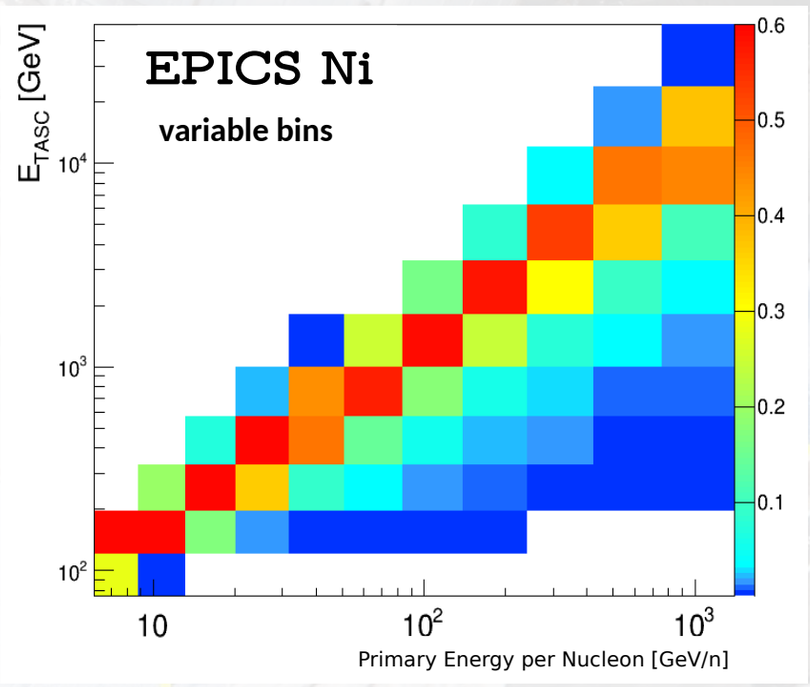

Two MC codes are used to estimate the energy response ("smearing") matrix, applying the same selection cuts as in the FD analysis: EPICS and FLUKA for Fe, EPICS and GEANT for Ni

(9) Systematic Errors: Iron

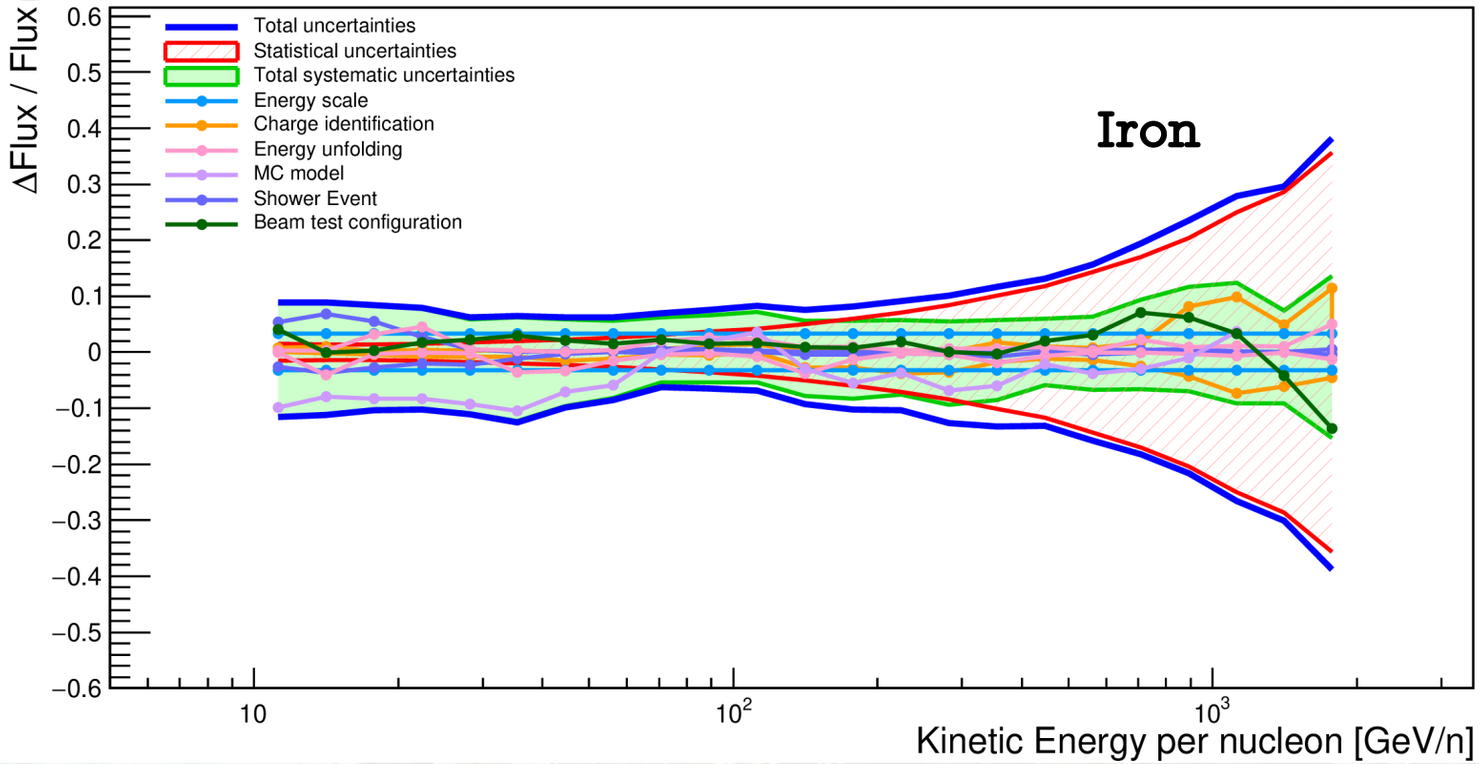

Energy-independent systematic uncertainties affecting the flux normalization include:

- **live time (3.4%)**
- **long-term stability (< 2%)**
- **geometrical factor (~1.6%)**

Systematic	Variation	Flux variation
Charge identification	Semiaxes of ellipse: up to ± 15%	Few % below 600 GeV/n, 10% @ 1 TeV
Energy Scale Correction	± 2% according to Beam Test	Rigid shift + 3.3%, -3.2%
Unfolding procedure	response matrix, varying spectral index from -2.9 to -2.2	Few %
MC Model	Energy response matrix with FLUKA	Up to 10% below 40 GeV/n, few % in the 100 GeV region, < 5% up to 1 TeV
Shower event	Different shape cut	5% below 30 GeV/n, 1% above
Beam test configuration	Beam test model configuration	Few %

(9) Systematic Errors: Nickel

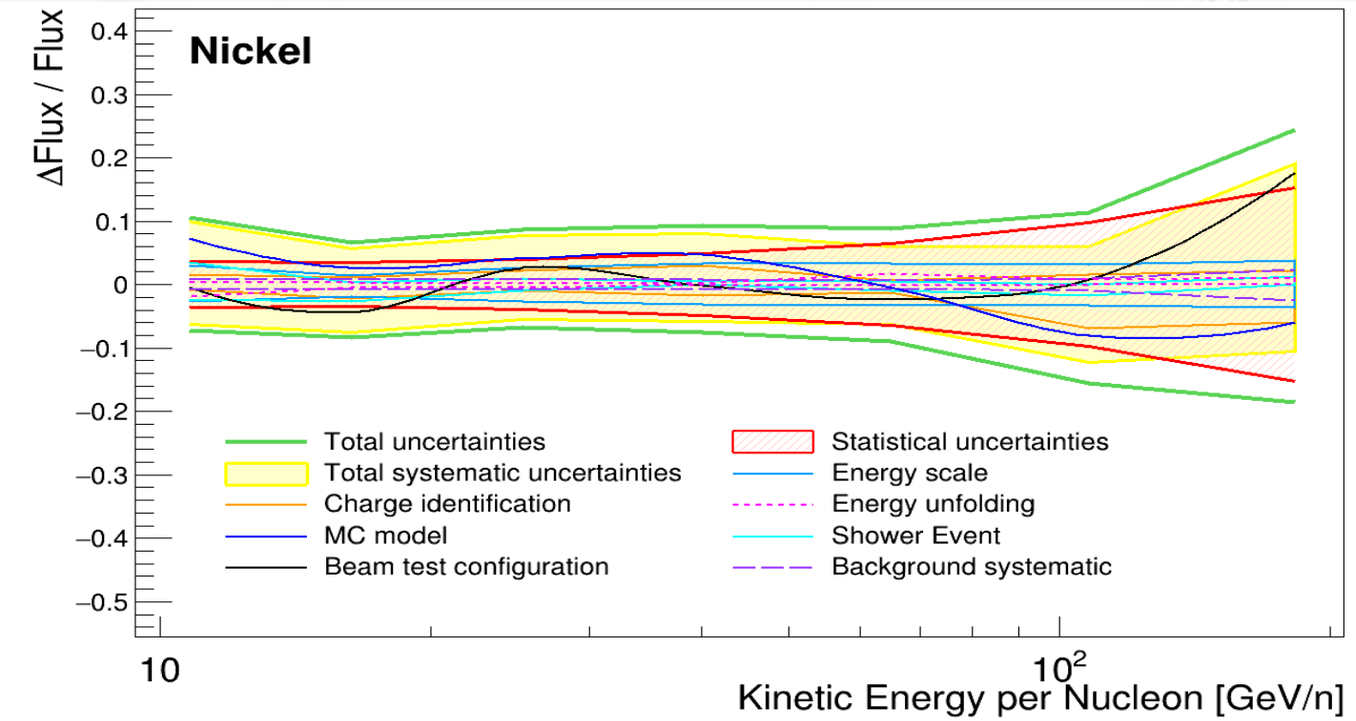

Energy-independent systematic uncertainties affecting the flux normalization include:

- **live time (3.4%)**
- **long-term stability (< 2%)**
- **geometrical factor (~1.6%)**

Systematic	Variation	Flux variation
Charge identification	Semiaxes of ellipse: up to ± 15%	Few % below 100 GeV/n, 8% @ 200 Gev/n
Energy Scale Correction	± 2% according to Beam Test	Rigid shift ±4%
Unfolding procedure	response matrix, varying spectral index from -2.9 to -2.2	Few %
MC Model	Energy response matrix with GEANT4	5% below 40 GeV/n, less than 5% in the 100—200 GeV/n region
Shower event	Different shape cut	4% around 10 GeV/n, 2% above
Beam test configuration	Beam test model configuration	Few %
Background systematic	Contamination level by as much as 50%	1% below 100 GeV/n, 3% at 200 GeV/n.

(10) Flux measurement

$$\Phi(E) = \frac{N(E)}{\Delta E \varepsilon(E) S\Omega T}$$

- N(E): bin counts of the unfolded energy distribution
- ΔE: energy bin width
- SΩ: geometrical acceptance
- T: live time
- ε(E): total selection efficiency

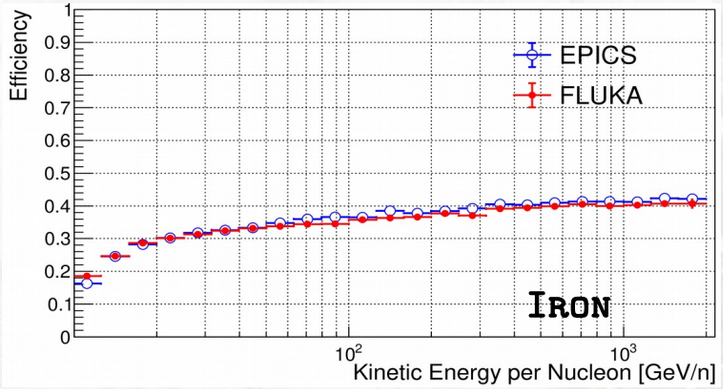

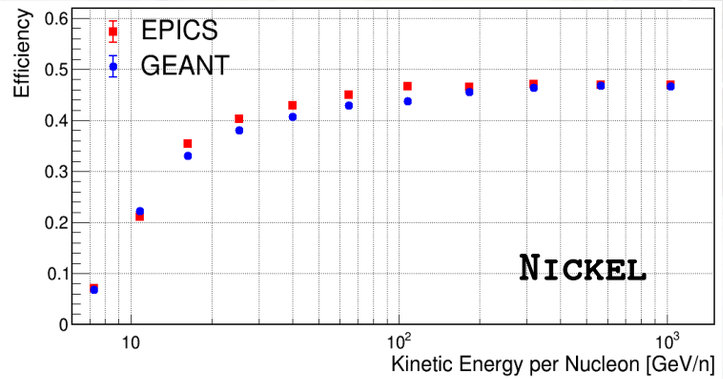

CALET Iron and Nickel Flux with multiplicative factor $E^{2.6}$

O. Adriani et al. *Phys. Rev. Lett.* **126** (2021) 241101

O. Adriani et al. *Phys. Rev. Lett.* ***128*** *(2022) 131103*

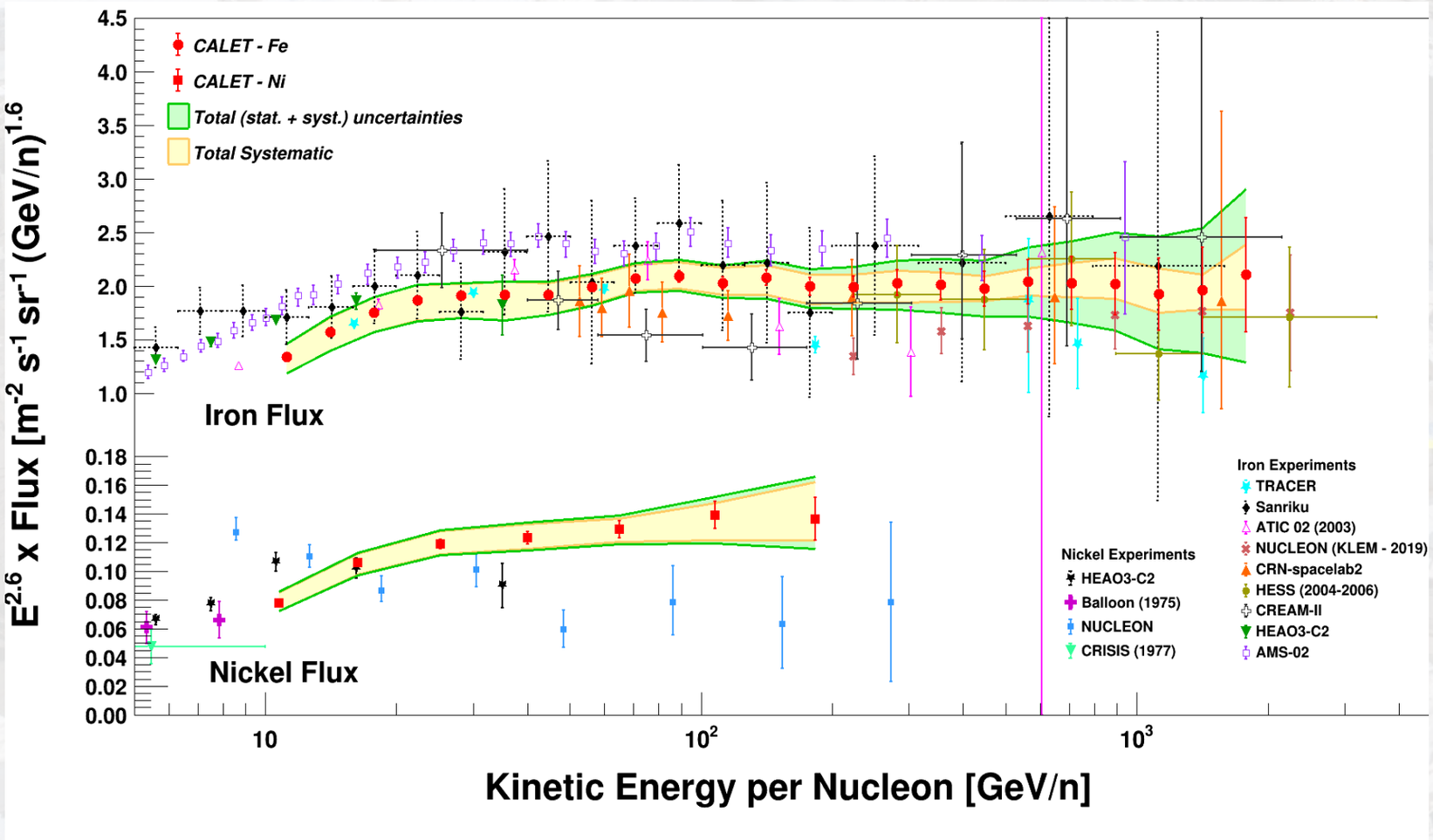

Spectral Index

Fit from 50 GeV/n to 2.0 TeV/n, with a single power law function

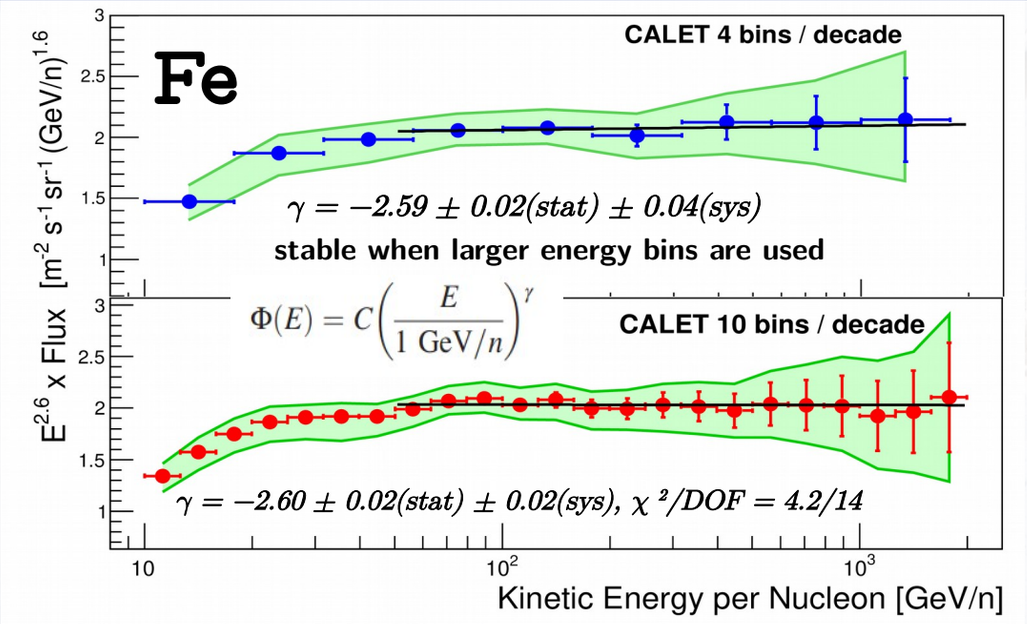

Sliding window

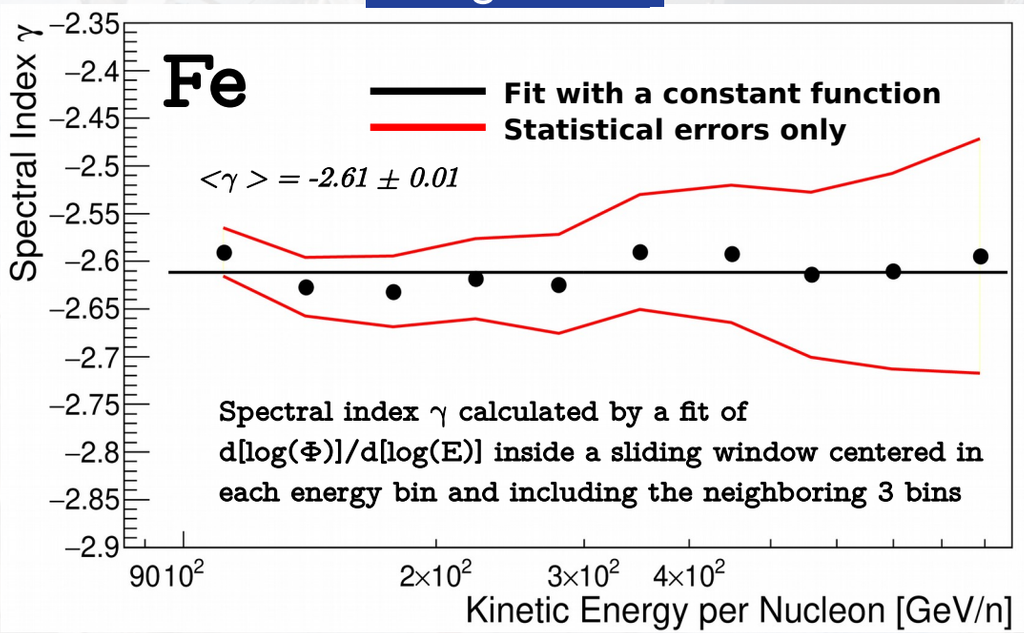

Fit from 20 to 240 GeV/n, with a single power law function

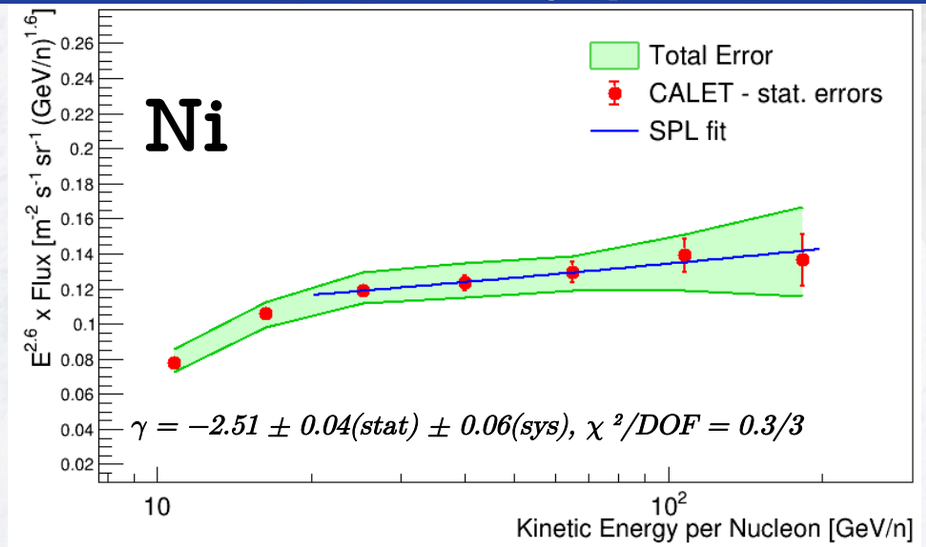

- Above 50 GeV/n the iron flux is compatible within the errors with a single power law.
- From 20 to 240 GeV/n the nickel flux is consistent with the hypothesis of an SPL spectrum

Nickel to iron ratio

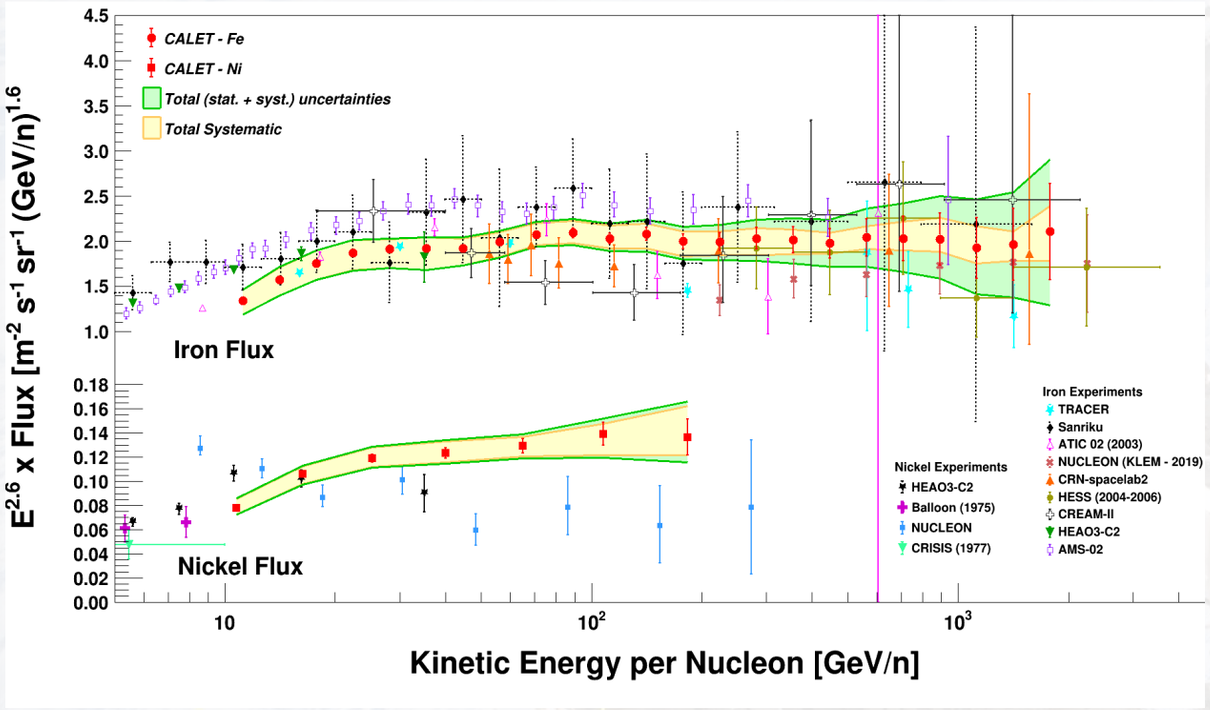

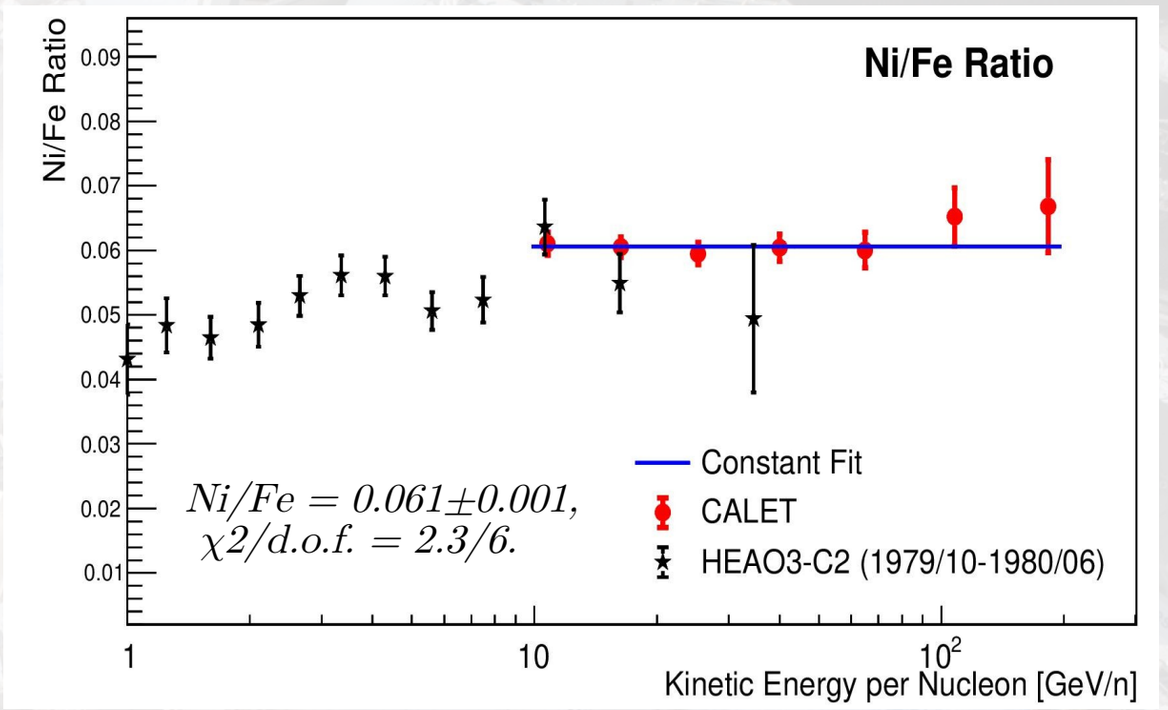

- The flat behavior of the nickel to iron ratio suggests that the spectral shapes of Fe and Ni are the same within the experimental accuracy
- This suggests a similar acceleration and propagation behavior as expected from the small difference in atomic number and weight between Fe and Ni nuclei

Conclusions

- The measurement of the energy spectra of iron and nickel with CALET from 10 GeV/n to 2.0 TeV/n and 8.8 to 240 GeV/n respectively, were performed with a significantly better precision than most of the existing measurements.

- CALET data turn out to be consistent with most of the previous measurements within the uncertainty error band, both in spectral shape and normalization. CALET and AMS-02 iron spectra have a very similar shape, but differ in the absolute normalization of the flux by ~20%.

- Below 20 GeV/n the nickel spectrum behavior is similar to the one observed for iron and lighter primaries.

- Above 50 GeV/n the iron spectrum is consistent with the hypothesis of a SPL spectrum up to 2 TeV/n with a spectral index value $\gamma = -2.60 \pm 0.03$.

- Above 20 GeV/n the nickel spectrum is consistent with the hypothesis of a SPL spectrum up to 240 GeV/n with a spectral index value $\gamma = -2.51 \pm 0.07$.

- The statistics and large systematic errors do not allow to draw a significant conclusion on a possible deviation from a single power law.

- The flat behavior of the nickel to iron ratio suggests that the spectral shapes of Fe and Ni are the same within the experimental accuracy. This suggests a similar acceleration and propagation behavior.

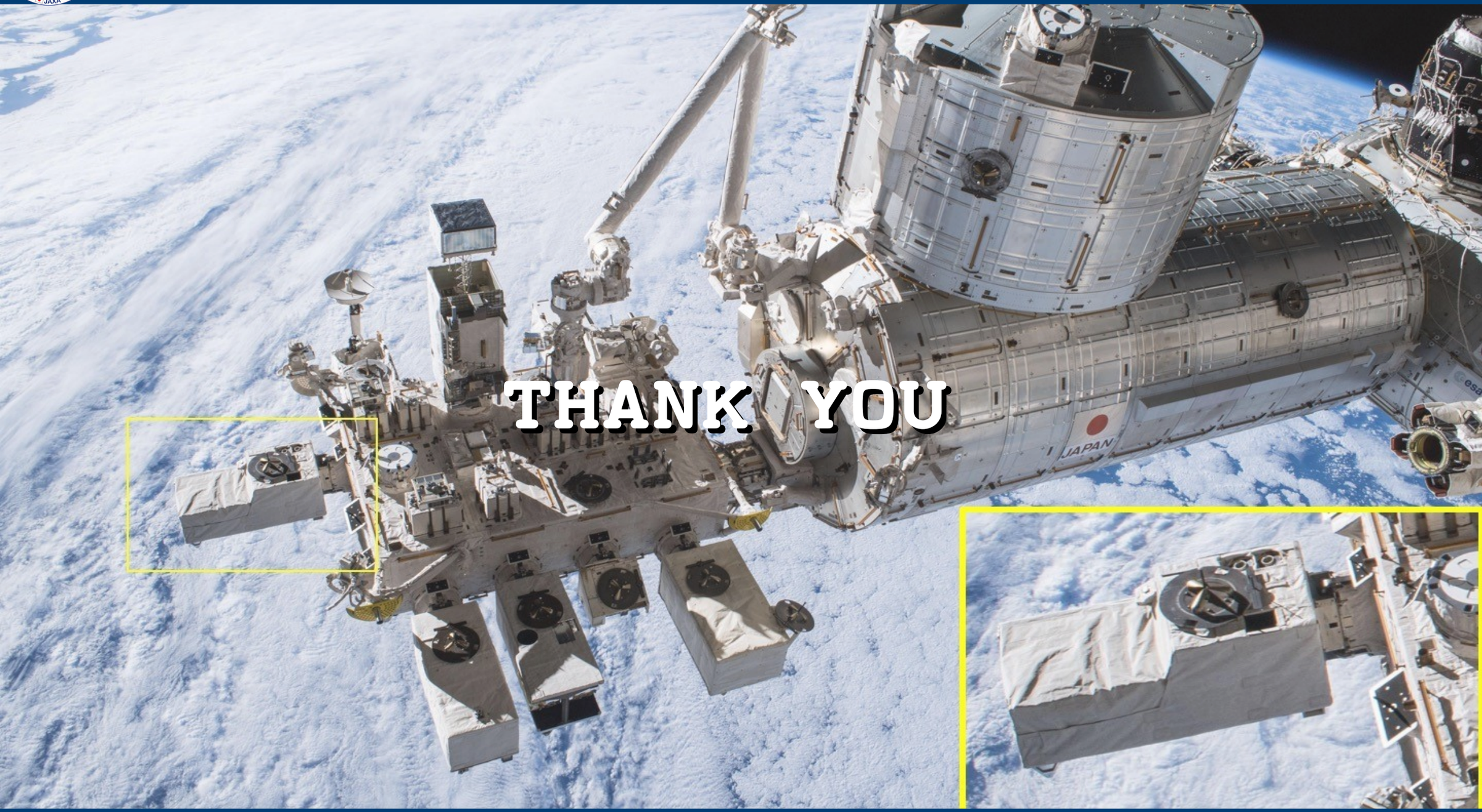

THANK YOU

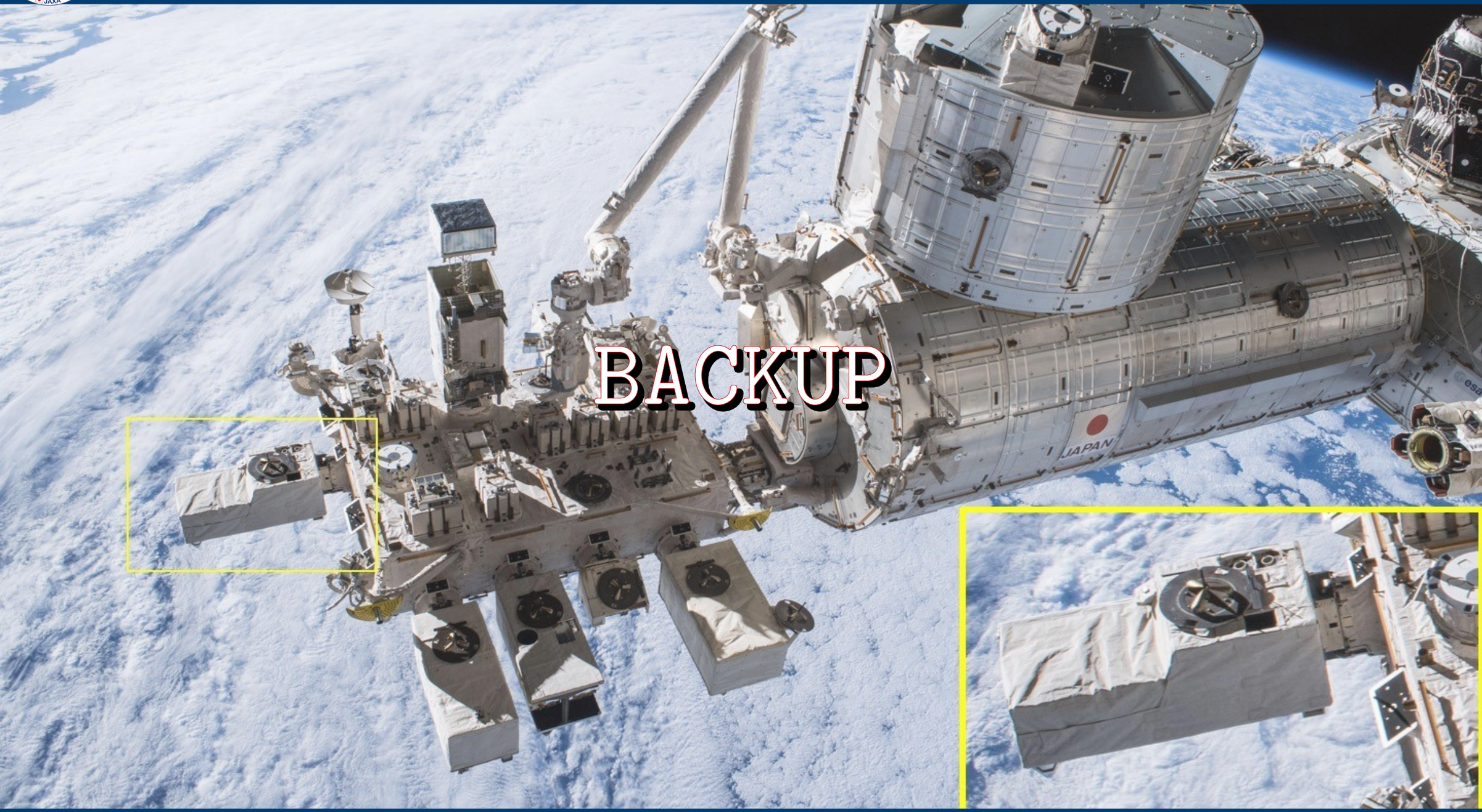
BACKUP

(1) (2) HET and Shower selection

- For light nuclei (Z<10), only events interacting in the detector are triggered.
- For heavy nuclei, the HET threshold is far below the signal amplitude expected from a particle at minimum ionization (MIP) and the trigger efficiency is close to 100%.

→ in order to select interacting particles, a deposit larger than 2 sigmas of the MIP peak is required in at least one of the first four layers of the TASC.

HE Trigger

Shower Event selection for Fe, Ni

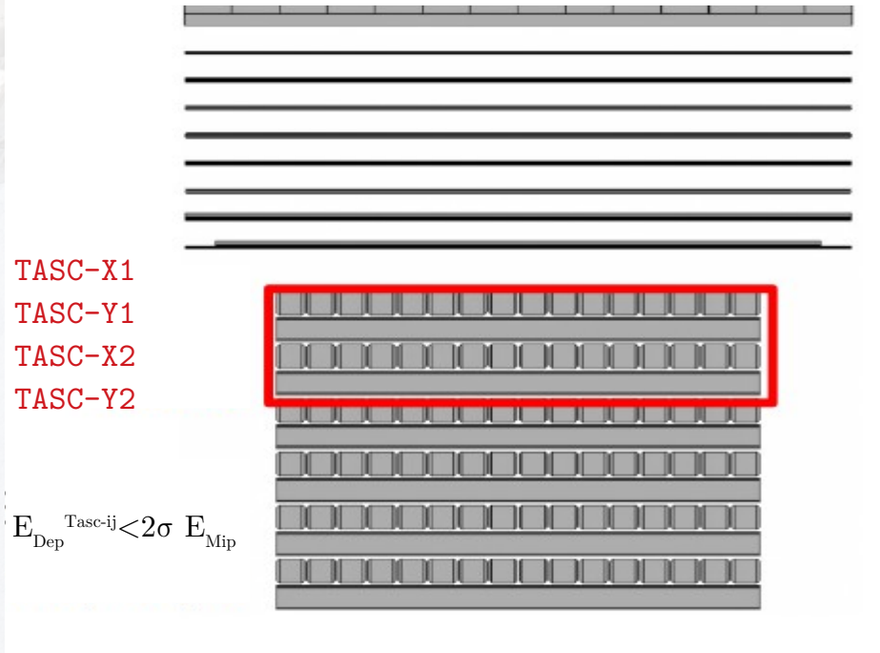

(3) (4) Tracking with IMC

Tracking algorithm based on a combinatorial Kalman filter

Tracking is used to:

- Determine cosmic ray (CR) arrival direction;
- Define geometrical acceptance;
- Identify CHD paddles and IMC scintillating fibers crossed by CR particle

Tracking performance for iron and nickel:

- angular resolution : ~0.08°
- spatial resolution for the impact point on the CHD: ~180 μm.

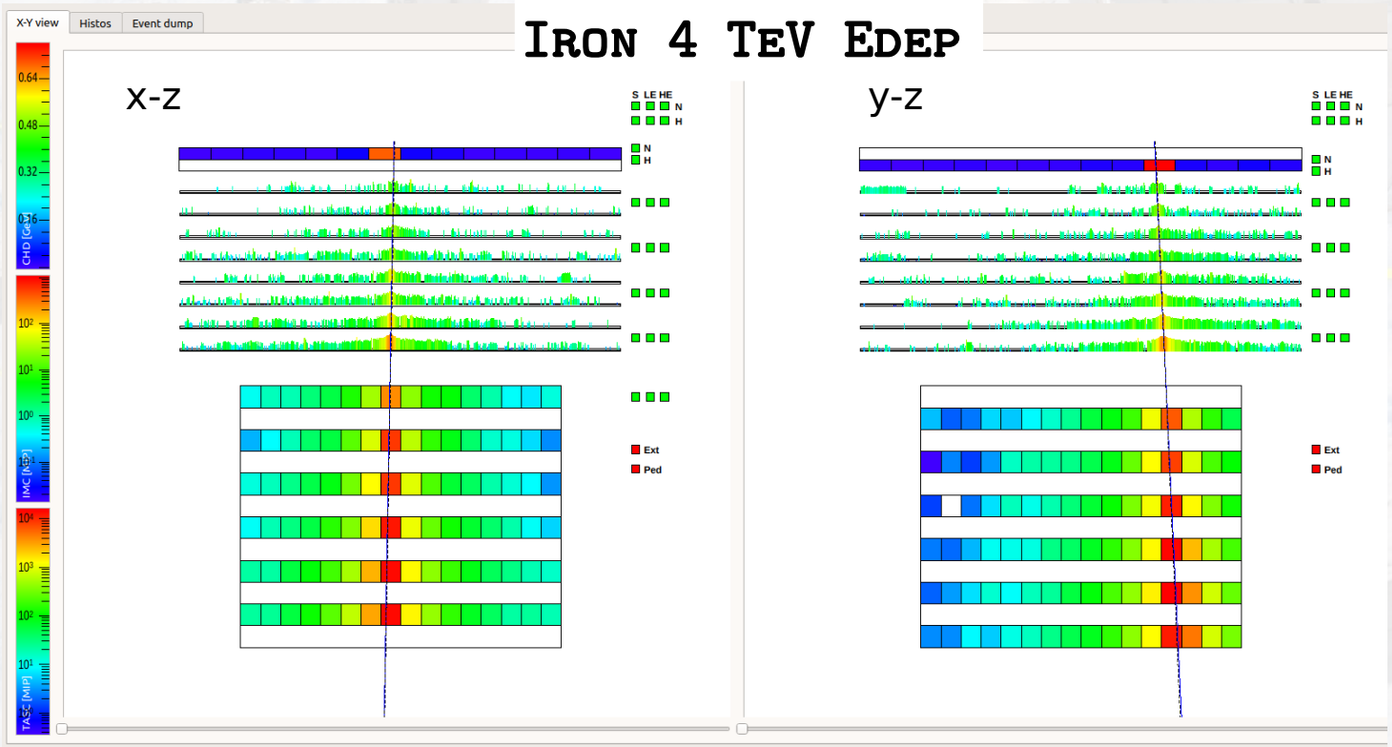

Beam Test Calibration

The energy response of the TASC derived from the MC simulations was tuned using the results of a beam test carried out at the CERN-SPS in 2015 with beams of accelerated ion fragments of 150 GeV/c/n.

- **Correction factors are:**
  - 6.7% for $E_{TASC} < 45$ GeV;
  - 3.5% for $E_{TASC} \geq 350$ GeV;
  - linear interpolation for $45 \leq E_{TASC} < 350$ GeV.

- **Good linearity up to maximum available beam energy (~6 TeV) between the observed TASC energy and the primary energy.**
- **Fraction of particle energy released in TASC is ~20%.**

- **Energy resolution around 30%.**

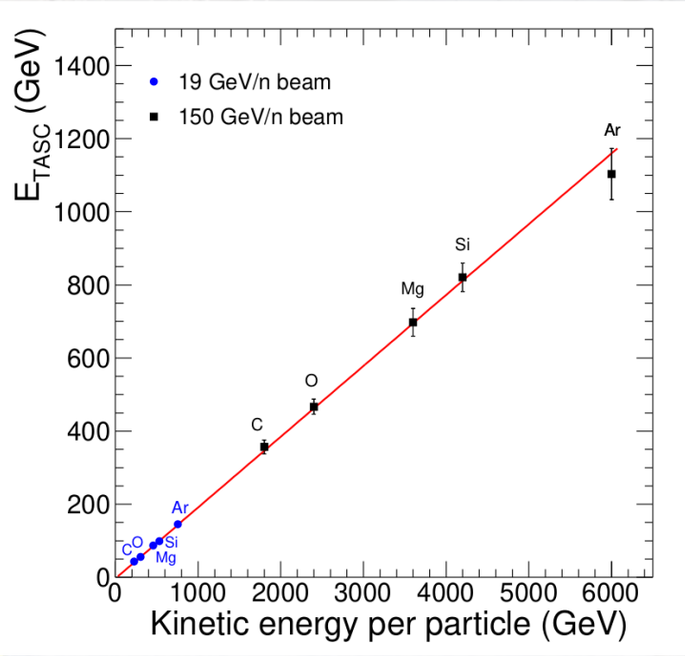

Fluxes normalization

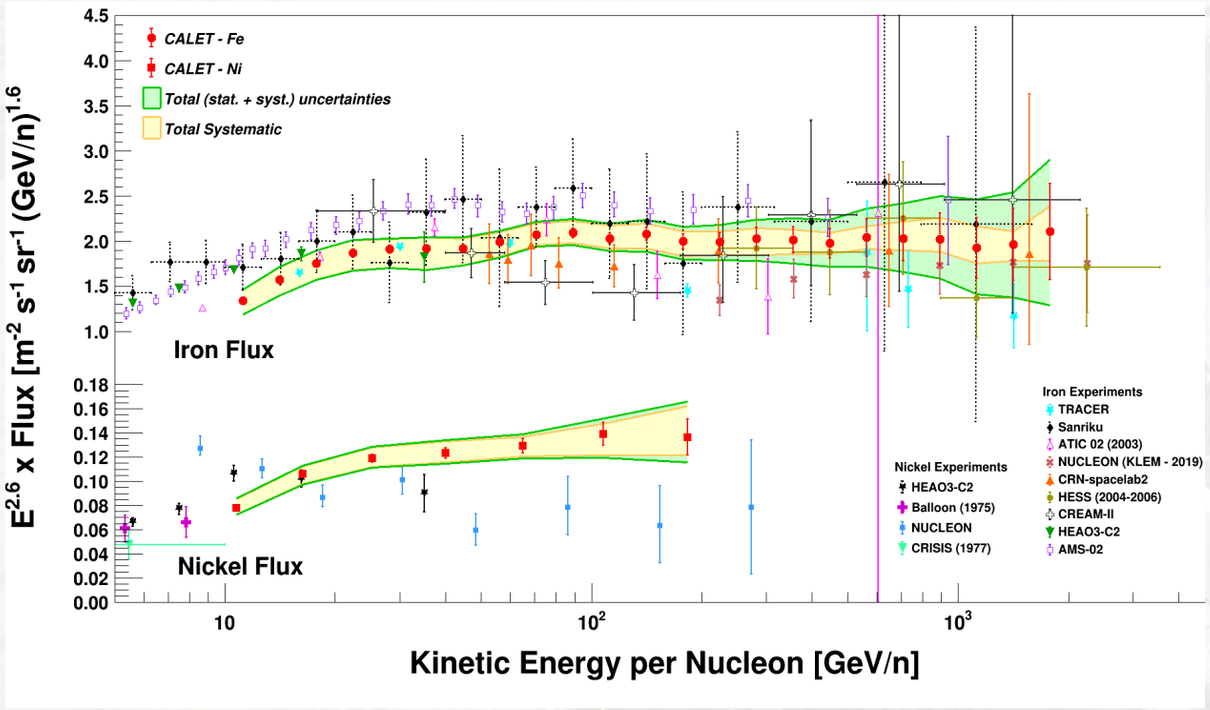

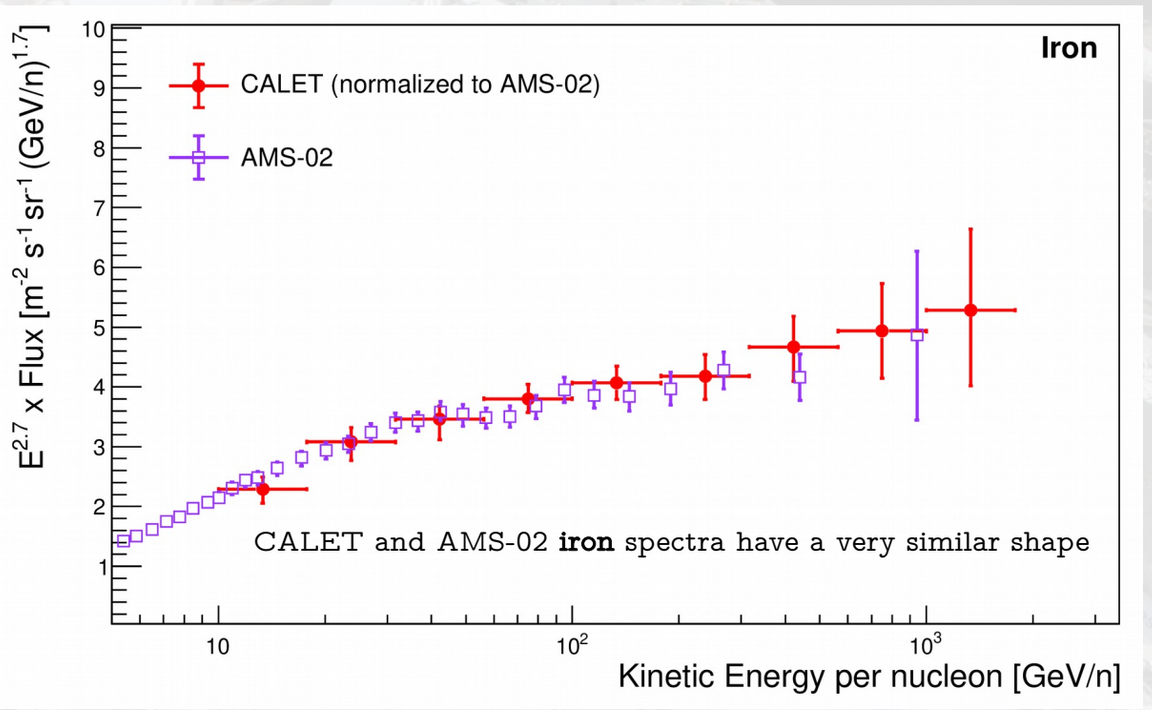

- CALET iron spectrum is consistent with ATIC 02 and TRACER at low energy
- CALET iron spectrum is consistent with CRN and HESS at high energy
- CALET and NUCLEON iron spectra have similar shape, but different normalization
- CALET and AMS-02 iron spectra have a very similar shape, but differ in the absolute normalization of the flux by ~20%

- CALET and HEAO3-C2 nickel spectra have similar flux normalization in the common interval of energies.
- CALET and NUCLEON nickel spectra differ in the shape although the two measurements show a similar flux normalization at low energy.

Bin Size

Different binning configurations were tested, obtaining similar smearing matrices and almost identical behavior in the final flux

Bin Size				
Iron	Standard: 10 equal log-bins	Test: 4 equal log-bins	Test: 5 equal log-bins	
Nickel	Standard: smoothly enlarged bins	Test: 3 equal log-bins	Test: 4 equal log-bins	Test: 5 equal log-bins

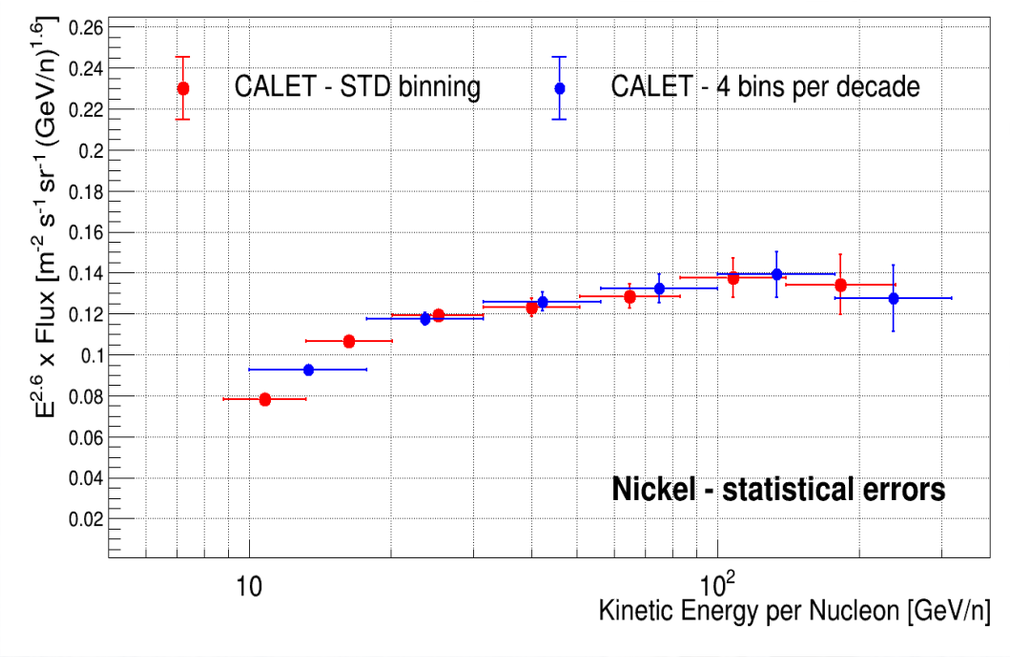

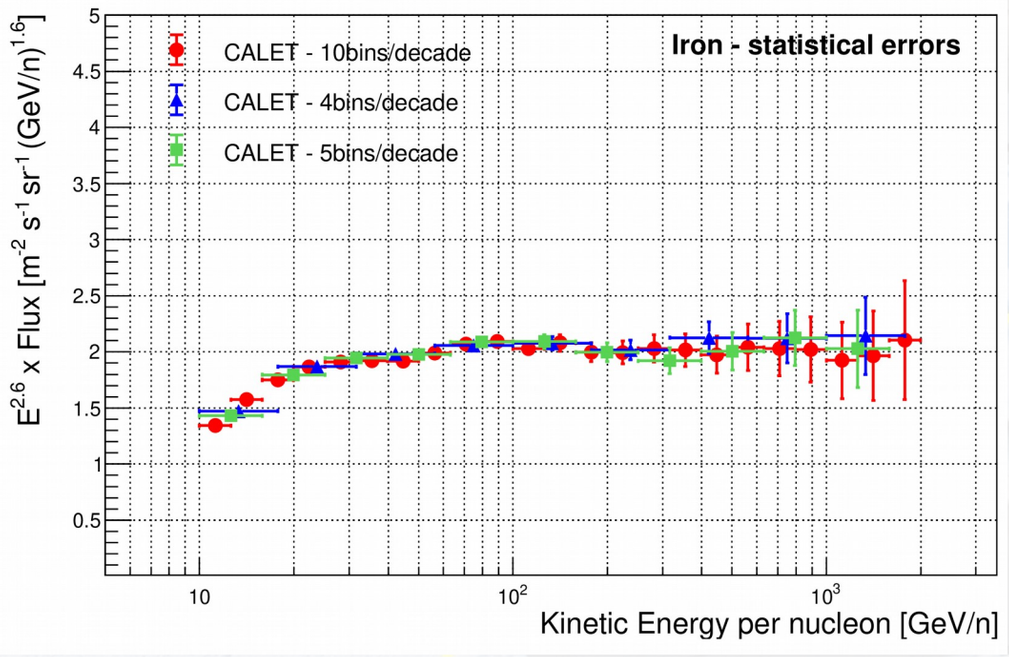

Within the errors, no statistically significant difference was found among the three fluxes

Interactions in the instrument

Amount of material above the CHD: 2 mm thick Al cover ($\sim 2.2\%\ X_0$ and $5 \times 10^{-3}\ \lambda_I$)

- the fraction of iron candidates tagged by both CHD layers among those detected by the top charge detector, was evaluated for MC and FD data.

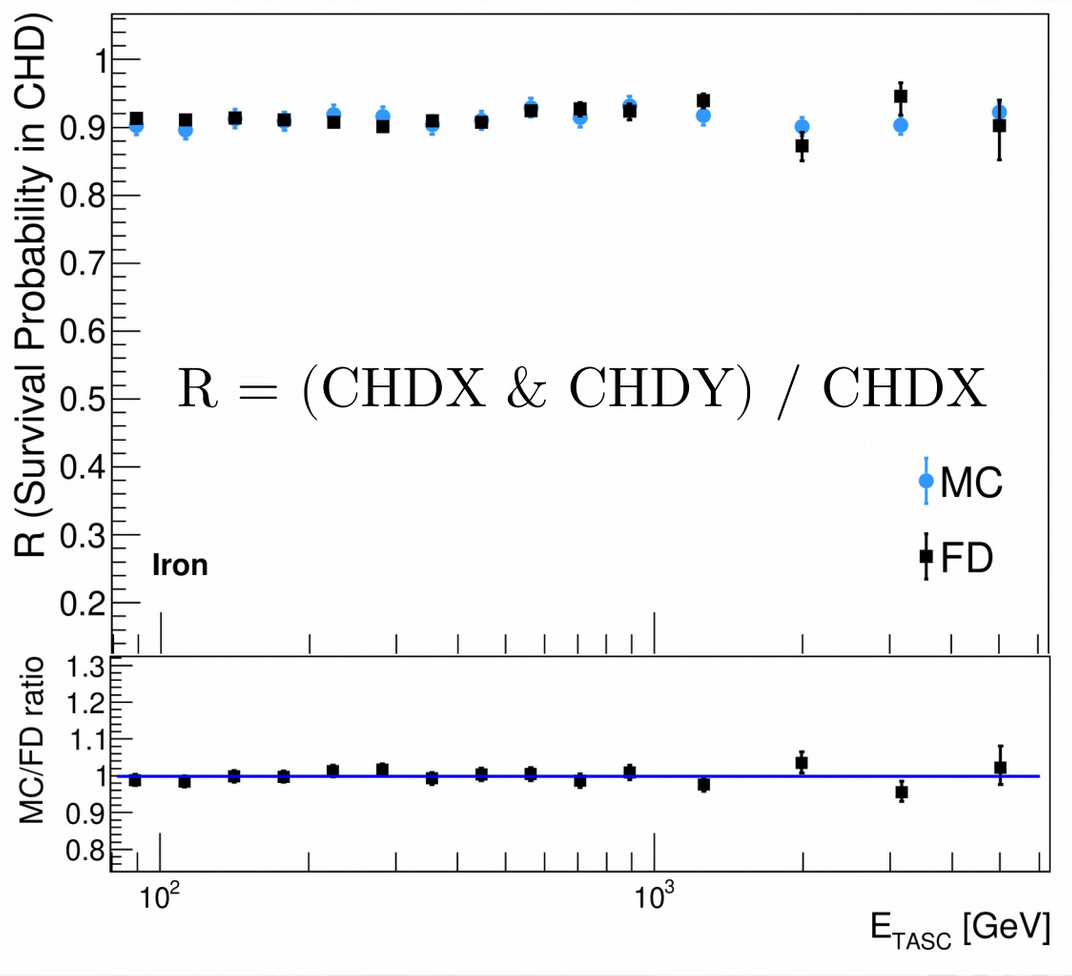

- good level of consistency between the MC and flight data, within the errors.

Total loss ($\sim$ 10%) of interacting iron events taken into account in the total efficiency.